MedChemComm

Efforts in Redesigning the Antileukemic Drug 6-Thiopurine: Decreasing Toxic Side Effects while Maintaining Efficacy

Journal:	*MedChemComm*
Manuscript ID	MD-RES-09-2018-000463.R3
Article Type:	Research Article
Date Submitted by the Author:	13-Dec-2018
Complete List of Authors:	Torres Hernandez, Arnaldo; Kansas State University, Chemistry Weeramange, Chamitha; Kansas State University, Chemistry Desman, Prathibha; Kansas State University, Chemistry Fatino, Anthony; Kansas State University, Chemistry Haney, Olivia; Kansas State University, Chemistry Rafferty, Ryan; Kansas State University, Chemistry

Efforts in Redesigning the Antileukemic Drug 6-Thiopurine: Decreasing Toxic Side Effects while Maintaining Efficacy

Arnaldo X. Torres Hernandez,[‡ab] Chamitha J. Weeramange,[‡b] Prathibha Desman,[b] Anthony Fatino,[b] Olivia Haney,[b] and Ryan J. Rafferty*[b]

[a]Department of Chemistry, Pontifical Catholic University of Puerto Rico, 2250 Boulevard Luis A. Ferré Aguayo, Suite 626 Ponce, PR 00717-0777

[b]Department of Chemistry, Kansas State University, 1212 Mid-Campus Drive North, Manhattan, KS 66506

‡These authors contributed equally to the work.

ABSTRACT

6-Thiopurine (6TP) is a currently prescribed drug in the treatment of diseases ranging from Crohn's disease to acute lymphocytic leukemia. While its potent mode of action is through incorporation into DNA as a thiol mimic of deoxyguanosine, severe toxicities are associated with its administration which hinder the potential therapeutic application. We have previously reported *in vitro* that the oxidative metabolites of 6TP, specifically 6-thiouric acid (6TU, K_i 7 μM), are potent inhibitors of UDP-glucose dehydrogenase (UDPGDH), an enzyme that is responsible for the formation of UDP-glucuronic acid (UDPGA), an essential substrate that is used in detoxification processes in the liver. An i*n vivo* investigation was undertaken to probe if 6TU inhibits UDPGDH in rat hepatocytes, and it was observed that 6TU does greatly suppress the conjugation of bilirubin with UDPGA. The failed excretion of bilirubin is linked to a majority of the reported toxicities associated with 6TP administration. Efforts were undertaken for the construction of 6TP analogs, substituted at the C8 position, to reduce inhibition of UDPGDH while retaining therapeutic efficacy. Three new 6TP analogs bearing a halogen (Br, Cl, and F) at the C8 position have been achieved over five-synthetic steps in overall yields of 16 to 32%. Each of these analogs were shown to have reduced inhibition towards UDPGDH, with K_i values of 192, 163, 215 μM, respectively. In addition, the bromine, chlorine, and fluorine analogs were shown to possess cytotoxicity towards the REH cell line (acute lymphocytic leukemia) having IC_{50} values of 9.54 μM (±0.97), 3.95 μM (±1.94), and 4.71 μM (±1.40), respectively. These three new 6TP analogs represent the first steps in the redesign of this potent anticancer agent into a better drug that possesses reduced toxic side effects while retaining therapeutic potency.

1. Introduction

6-Thiopurine (6TP, **1**) has been a continuously prescribed therapeutic since its FDA approval in 1952, shortly after its discovery in 1950 by Gertrude Elion and George Hitchings at Burroughs Wellcome.[1] This potent therapeutic serves as a treatment option for numerous diseases, such as, but not limited to: acute lymphocytic leukemia (ALL),[2, 3] non-Hodgkin's leukemia,[4, 5] Crohn's disease,[6-8] and inflammatory bowel disease.[9, 10] 6TP has no therapeutic properties itself, however, it is metabolized into a therapeutic form, a deoxyguanosine nucleotide mimic, commencing with the phosphoribosylation by hypoxanthine-guanine phosphoribosyltransferase (HGPRT) forming the nucleotide mimic 6-thioinosinic acid monophosphate (TIMP, **2**). HGPRT is an enzyme that usually catalyzes phosphoribosylation of hypoxanthine (C6 hydroxyl) to inosinic acid (IMP).[11] Oxidation of the C2 position of 6TP is accomplished by inosine-5'-monophosphate dehydrogenase (IMPD), an enzyme that is overexpressed in the presence of 6TP, followed by C2 amine installation by guanine monophosphate synthase (GMPS) giving rise to either thioguanosine mono phosphate (TGMP or dTGMP, **3**).[11-13] Multiple kinase transformations then afford dTGTP (**4**), which gets incorporated into DNA in place of dGTP. However, incorporation of dTGTP does not immediately result in apoptosis, via base pair mismatching, but requires multiple passages through the S-phase allowing for sufficient dTGTP incorporation into DNA.[14] It has also been shown that 6-thioguanine (6TG, **5**) can be used in conjunction with 6TP and is acted upon by HGPRT accessing the monophosophate nucleotide formed via 6TP metabolism.

Checkpoint activation is required for recognition of the mismatched base pairing within DNA post **4** incorporation; a process commonly suppressed within cancer cells.[15-17] Mutually 6TP and 6TG can be methylated to form the corresponding thiol ethers by thiopurine methyltransferase (TPMT), neither possessing any cytotoxic properties, but do induce checkpoint activation.[18]

Additionally, TIMP (**2**) can be transformed into its corresponding methyl thiol ether, but rather than activating checkpoints this species has been proven to inhibit *de novo* purine biosynthesis.[19] This inhibition allows for the cellular uptake of purines to increase, including 6TP, which corresponds to a higher probability of dTGTP incorporation into DNA that can then lead to apoptosis, via base pair mismatching.

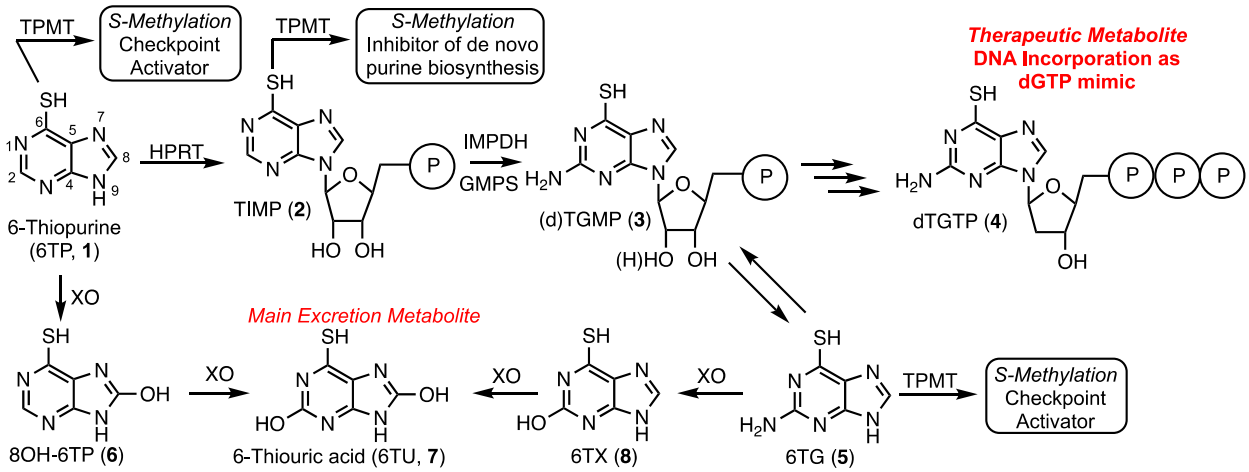

Fig. 1 Metabolism of 6-Thiopurine: 1) Therapeutic pathway forming dTGTP, a dGTP mimic, which incorporates into DNA resulting in apoptosis, and 2) the excretion pathway allowing for the removal of 6-thiopurine and its biosynthetic metabolites.

In parallel to 6TP's therapeutic metabolism, efficient oxidative pathways remove 6TP from the body, thereby decreasing its therapeutic potential. Xanthine oxidase (XO) can directly oxidize the C8 position of 6TP forming 8-OH-6TP (**6**), a species that is not a substrate for HGPRT, thus, eliminating any therapeutic potential.[20] Moreover, **6** can be further oxidized at the C2 position forming 6-thiouric acid (6TU, **7**), which is the terminal excretion metabolite. This highly efficient oxidation by XO limits the bioavailability of 6TP. In route to dTGTP (**4**), dTGMP (**3**) can be formed into 6TG, which is rapidly oxidized to 6-thioxanthine (6TX, **8**), a species that is further

oxidized by XO to 6TU. Once 6TU is formed, it is well retained by the body beyond 24-hours post-6TP administration.[20]

As with nearly all therapeutic drugs, the benefits come with side effects that limit effectiveness and general applications. 6TP is not immune to this trend, with multiple toxicities associated with its use including, but not limited to: pulmonary lesions, myocarditis, reticulocytopenia, depletion of cellularity in bone marrow, intestinal ulcerations, jaundice, hepatotoxicity, and even death.[13, 15] Of these, the most predominate toxic side effects are jaundice and hepatotoxicity, corresponding to the reported increase in bilirubin levels within patients taking 6TP. In addition to the toxicities listed above, increased bilirubin levels within the body can cause hyperbilirubinemia, kernicterus, Crigler-Najjar syndrome, Gilbert's syndrome, liver failure, and death.[21-23] While 6TP is a currently prescribed anticancer agent, its toxic side effects are so potent and prevalent that the administration of 6TP is given in an on/off strategy, allowing time for the toxic species to be cleared by the body. Unfortunately, this greatly reduces its therapeutic efficacy, restricts the quality of life of the patients taking the drug, and has ultimately limited its use as an anticancer therapy. Our laboratory is interested in repurposing dismissed or under-utilized anticancer therapies, such as 6TP. Noting the common connection between the predominate toxic side effects possibly originating in the bilirubin pathway, this prompted us to begin a systematic study to explore the effects of 6TP and its oxidative metabolites.

The bilirubin pathway refers to the excretion of bilirubin from the body through detoxification in the liver.[24-26] Heme groups are released when red blood cells undergo senescence, which in the presence of oxygen and NADPH, reduces the heme to bilirubin (**11**, also referred to as unconjugated bilirubin, UCB).[24] Bilirubin is a relatively large non-polar compound that is not easily excreted by the body (Figure 2A).[27] The excretion of bilirubin is achieved through

conjugation by UDP-glucuronyl transferase (UGT-1A) with two UDP-glucuronic acids (UDPGA, **10**) forming bilirubin diglucuronide (BDG, **12**), a water-soluble and excretable compound.[28, 29] Physiologically, UDPGA (**10**) is formed from the oxidation of UDP-glucose (UDPG, **9**) via UDP-glucose dehydrogenase (UDPGDH).[30] We have reported that 6TP and its excretion/oxidative metabolites inhibit UDPGDH, but not UGT-1A (Figure 2B).[31] Furthermore, *in vitro* investigations revealed that 6TP and its excretion metabolites resulted in an increase in bilirubin and a decrease in conjugated bilirubin levels, relative to controls. While 6TP was shown to have low inhibition towards UDPGDH, its main excretion metabolite 6TU has a 41-fold increase in inhibition. Noting that the formation of 6TU via XO is rapid, we were led to investigate the other oxidative metabolites. Investigations of 6-thioxanthine (**8**, C2 hydroxyl) revealed a five-fold increase in inhibition towards UDPGDH and 8-OH-6TP a 20-fold increase in inhibition, relative to 6TP. From this, it is suggested that the C8 position is critical in the inhibition properties towards UDPGDH.[31] As such, we propose that analogs that block the C8 position of 6TP, thereby preventing oxidation by XO to the C8-OH, will limit, if not eliminate, inhibition of UDPGDH. We speculate that the reduced inhibition of UDPGDH will result in a higher concentration of the UDPGA liable pool to allow for conjugation of bilirubin and its excretion, thereby reducing one of the predominate toxic side-effects of 6TP administration.

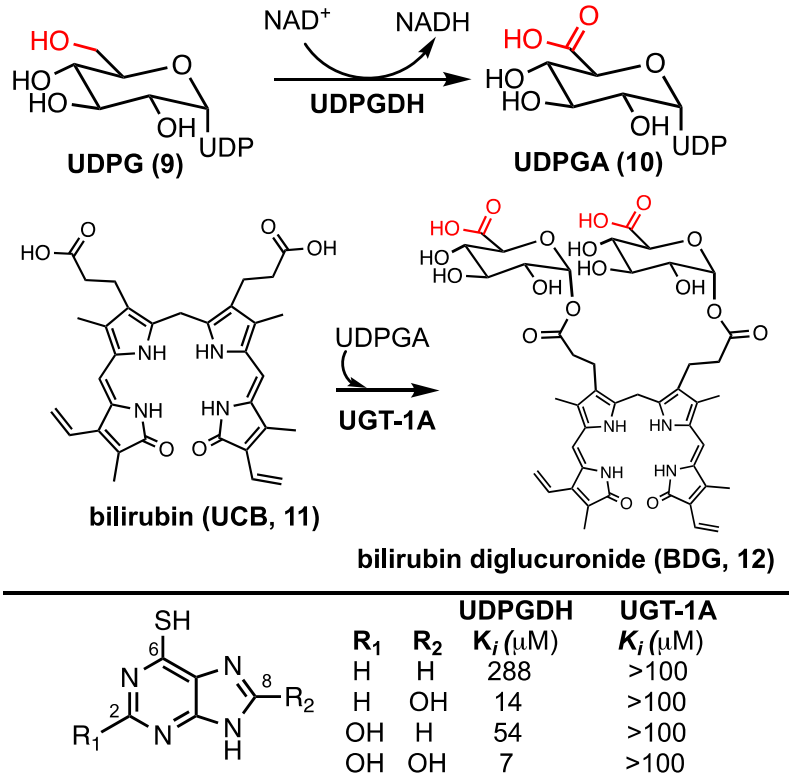

		UDPGDH	UGT-1A
R_1	R_2	K_i (μM)	K_i (μM)
H	H	288	>100
H	OH	14	>100
OH	H	54	>100
OH	OH	7	>100

Fig. 2 (Upper) Biosynthesis of UDPGA from the oxidation of UDPG by UDPGDH and conjugation of bilirubin with UDPGA by UGT-1A forming the excretable bilirubin diglucuronide. (Lower) Inhibition profiles of 6TP and excretion metabolites towards UDPGDH and UGT-1A.

Fig. 2 (Upper) Biosynthesis of UDPGA from the oxidation of UDPG by UDPGDH and conjugation of bilirubin with UDPGA by UGT-1A forming the excretable bilirubin diglucuronide. (Lower) Inhibition profiles of 6TP and its excretion metabolites towards UDPGDH and UGT-1A.

2. Results and discussion

2.1 Hepatotoxicity Evaluation of 6-Thiopurine and 6-Thiouric acid

Previously, our lab has shown that the excretion metabolites of 6TP, specifically those hydroxylated at both, or either, C2/8, possess inhibition towards UDPGDH but not UGT-1A, when both enzymes were screened independently *in vitro* .[31] To further corroborate these findings and to give a potential correlation to *in vivo* effects, we set forth to investigate our initial claim that 6TP and 6TU inhibit UDPGDH in a bio-mimic *in vivo* assay, via isolated perfused livers of rat

hepatocytes. While it is difficult to correlate the exact enzyme being inhibited by a small molecule in a whole cell experiment, we decided to explore UDPGDH inhibition with regards to these two steps through quantification of the glucuronidated bilirubin species. Full glucuronidation of UCB leads to the formation of BDG (**12**, Figure 2), however monoglucuronidation results in two different monoglucuronidated bilirubin species (BMG1 and 2); in this work, both BMG1 and 2 were quantified together (herein refered to as BMG). Rat liver hepatocytes were used for the assessment of formation of BMG and BDG in the presence of 6TP and 6TU at high and low concentrations. Table 1 shows the quantification of UCB, BMG, and BDG in hepatocytes. Quantification of the bilirubin species throughout this study is normalized to the BMG levels of the control set.

Table 1 Hepatocyte studies with 25 and 50 μM of 6TP and 5 and 10 μM of 6TU. Each group is an average of three independent runs with standard error bars shown.

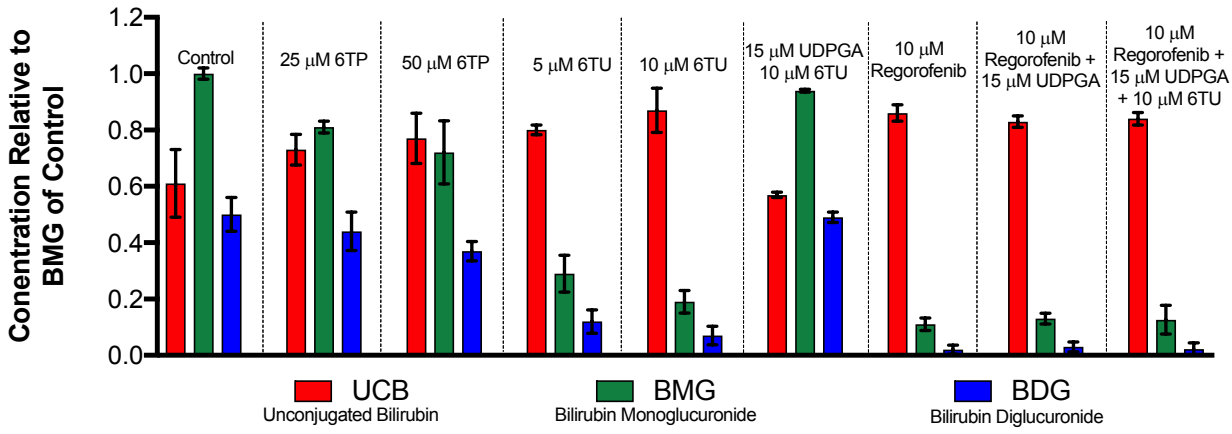

Subjecting the harvested hepatocytes to 25 μM 6TP showed an overall decrease in the conjugation of UCB and formation of BDG; relative to the control set, UCB levels increased by 19%, and both BMG and BDG levels were decreased by 19% and 12%, respectively. Based upon our previous conducted *in vitro* assays, this finding was not unexpected and further supports that

inhibition of UDPGDH is responsible for the decrease in bilirubin conjugation and subsequent toxicity. Increasing the dosage of 6TP to 50 μM revealed greater decrease in BMG and BDG levels, 28% and 26%, respectively, relative to controls. The observed decrease in BMG and BDG levels is assumed to arise from the increased conversion of 6TP to 6TU via XO, thereby inhibiting UDPGDH. Treatment with 5 and 10 μM of 6TU revealed potent inhibition of BMG and BDG formation, far greater than when 6TP was administered. When 5 μM of 6TU was employed an increase of 31% in UCB levels was observed, relative to the controls. Furthermore, BMG and BDG levels decreased by 71% and 76, respectively. The levels of BMG formation decreased by 81% and BDG levels by 86% when 10 μM of 6TU was used, with an increase in UCB levels by 42%, all relative to the controls. If the reduced BDG formation does originate from the decrease in the liable pool of UDPGA, addition of UDPGA to the system should allow recovery of the system similar to the controls. The addition of 15 μM of UDPGA along with 10 μM of 6TU resulted in the production of BDG levels similar to that of the control group, suggesting that 6TU does suppresses the formation of UDPGA via inhibition of UDPGDH *in vivo* but does not inhibit UGT-1A, but does require further investigations into UGT-1A itself is required to substantiate this claim.

Treatment with 10 μM regorafenib, a known inhibitor of UGT-1A and proven non-inhibitor of UDPGDH by our group (see Supplementary Information), resulted in strong inhibition in the formation of both BMG (89% decrease) and BDG (96% decrease) is observed, both greater than 6TU. When treated with 10 μM regorafenib and 15 μM of UDPGA a similar pattern of reduced BMG and BDG formation is observed. Furthermore, treatment with 10 μM of regorafenib, 10 μM 6TU, and 15 μM of UDPGA also showed the same profile of BMG and BDG levels. Thus, the

decrease in BMG and BDG levels from regorafenib are from UGT-1A inhibition, which can be translated into confirming that the effects of 6TP and 6TU are upon UDPGDH and not UGT-1A.

With the confirmation of *in vivo* inhibition of UDPGDH by 6TP and 6TU, the latter being more potent with regards to suppressing BDG formation, the construction of 6TP analogs was considered the next logical step. From previously conducted *in vitro* investigations, it was observed that hydroxylation upon the C2 and C8 positions does translate into inhibition of UDPGDH.[31] The C2 position of 6TP cannot be modified as amine installation post phosphoribosylation is required to form its therapeutically active form; therefore, modification of the C8 position is considered the only viable strategy for analog construction.

2.2 Chemistry

Construction of C8-substituted purine systems is reported in the literature,[32, 33] however the inclusion of the C6 thiol with C8 substitution, restricted to alkyl and phenyl analogs, is limited. In the efforts to construct analogs that block the C8 position from oxidation by XO, we set forth to construct analogs that bear halogens about the C8 position in hopes of retaining the therapeutic character of 6TP. Halogens were chosen for the C8 substitution, rather than alkyl or aryl substituents, to decrease the probability of failed DNA incorporation due to sterics about the C8 position. Starting from the commercially available 6-chloropurine (**13**), protection of the N9 nitrogen was successfully accomplished with potassium carbonate and *para*-methoxybenzyl chloride (PMBCl) to access **14** in 58% yield (Scheme 1), matching reported characterization found in the literature.[34-36] In addition to obtaining pure **14**, these conditions also allow access to the N7 PMB protected compound (**15**) in 34% yield. Further synthetic elaborations were conducted upon **14** but not **15**. While **15** can be employed in the efforts of accessing C8 halogen 6TP analogs in the same route as **14**, there is a decrease in yields using this material and will be discussed below.

With **14** in hand, efforts towards the installation of halogens (bromine,[37, 38] chlorine,[34] and fluorine[39]) at the C8 position were undertaken through modifications of reported procedures. Deprotonation of the C8 hydrogen of **14** was accomplished with freshly prepared LDA; the lithiated species was then treated with 1,2-dibromotetrachloroethane to access the C8-bromo compound (**16a**) in 75% yield. The substitution of the 6-chloro group upon purines has precedent in the literature,[40, 41] following these reported procedures, thiol installation with thiourea and ethanol reflux, afforded **17a** in 92% yield over two-steps. Deprotection of the PMB protecting group was performed by refluxing sulfuric acid, thus, gaining access to the 8-bromo-6TP (**18a**) in 81% yield, with an overall 32% yield over five synthetic transformations from **13**. Additional 8-Br-6TP (**18a**) was accessed from **15** by subjecting it to the same conditions with comparable yields, except about the thiol installation step. From the N7-PMB variant of **16a**, subjection to thiol installation provided a 58% yield. It is thought that the additional steric congestion brought from the N7 PMB is the cause for the decrease in yields, as nearly 34% of starting material is recovered.

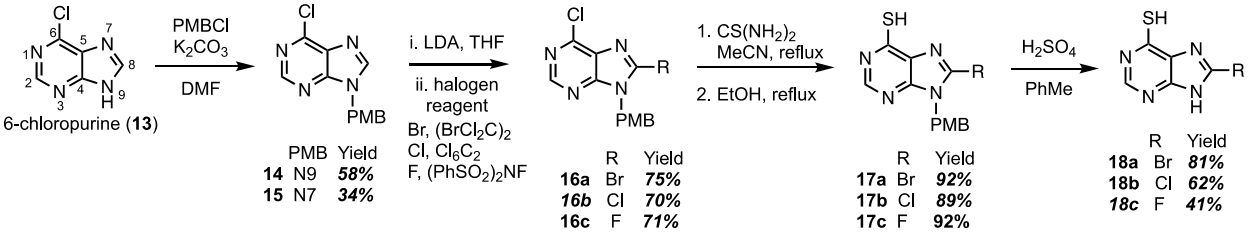

Scheme 1 Synthetic route accessing the bromo-, chloro-, and fluoro-C8-substituted 6TP analogs from 6-chloropurine.

Following the same approach described in Scheme 1, accessing the C8 chloride and fluoride analogs were undertaken. Deprotonation of the C8 hydrogen of **14** was accomplished with LDA and subsequent treatment with hexachloroethane afforded 6,8-dichloro-*N*-

paramethoxbenzylpurine (**16b**) in 70% yield. In an analogous fashion, treatment with N-fluorobenzenesulfonimide (NFSI) afforded **16c** in 71% yield, with 19% of starting material recovered. Thiol installation was performed upon **16b** and **16c** accessing **17b** and **17c** in 89% and 92% yields, respectively. When the same transformation was attempted upon the N7 variants, a suppression in yields were obtained similar to the bromine analog described previously. Removal of the PMB group was performed under refluxing sulfuric acid to give access to **18b** and **18c** in 62% and 41% yields. The chloro- and fluoro-analogs were constructed over five-steps in overall yields of 22% and 16%, respectively.

2.3 Biological evaluation of 6TP analogs

Inhibition assessment of the synthesized C8-halogenated 6TP analogs was performed independently against the two enzymatic steps of the bilirubin pathway, UPDGDH and UGT-1A. A cytotoxicity assessment was performed against the acute lymphocytic leukemia cell line REH as well.

2.3.1 Inhibition Evaluation Towards UDPGDH

To investigate the inhibition properties of the analogs towards UDPGDH, a previously disclosed and employed UV/Vis method was used.[31] Recalling the potent inhibitory properties of the C2 and/or C8 hydroxylated 6TP excretion metabolites towards UDPGDH, we were surprised to find that each of the analogs possess minimal inhibition (Table 2-D). The C8 bromine analog was observed to inhibit UDPGDH with a K_i of 192 μM, the C8 chlorine analog was shown to have the strongest inhibition of the C8 halogenated 6TP analogs with a K_i of 163 μM, and the C8 fluorine analog the weakest inhibition with an observed K_i of 215 μM (Table 2 A-C). Previously, we reported a K_i of 288 μM for 6TP towards UDPGDH, and relative to the analogs synthesized a similar weak inhibition profiles were observed. While the minimal inhibition possessed by the

three newly constructed analogs towards UDPGDH represent a positive step in eliminating the toxicity associated with 6TP, further evaluation towards UGT-1A is required, as is assessment on whether these analogs retain a similar cytotoxicity comparable to 6TP.

Table 2 Inhibitor assessment towards UDP-glucose dehydrogenase *in vitro* by C8-halogenated 6TP analogs through Lineweaver-Burk plot analysis under UDPG varying NAD^+ saturating conditions. A) Concentration of 8-Br-6TP, varying UDPG, screened were 0, 50, 75, 100 μM with the calculated slopes of each line equaling 0.098, 0.121, 0.132, 0.153, respectively. Plotting slopes versus concentration gave a regression line of y=0.0005x+0.096. B) Concentration of 8-Cl-6TP, varying UDPG, screened were 0, 50, 75, 100 μM with the calculated slopes of each line equaling 0.097, 0.129, 0.137, 0.156, respectively. Plotting slopes versus concentration gave a regression line of y=0.0006x+0.098. C) Concentration of 8-F-6TP, varying UDPG, screened were 0, 50, 75, 100 μM with the calculated slopes of each line equaling 0.106, 0.132, 0.145, 0.152, respectively. Plotting slopes versus concentration gave a regression line of y=0.0005x+0.108. D) Summary of previously determined K_i values towards UDPGDH for 6TP and its excretion metabolites; summary of the found K_i of synthesized analogs. Each group is an average of three independent runs with standard error bars shown.

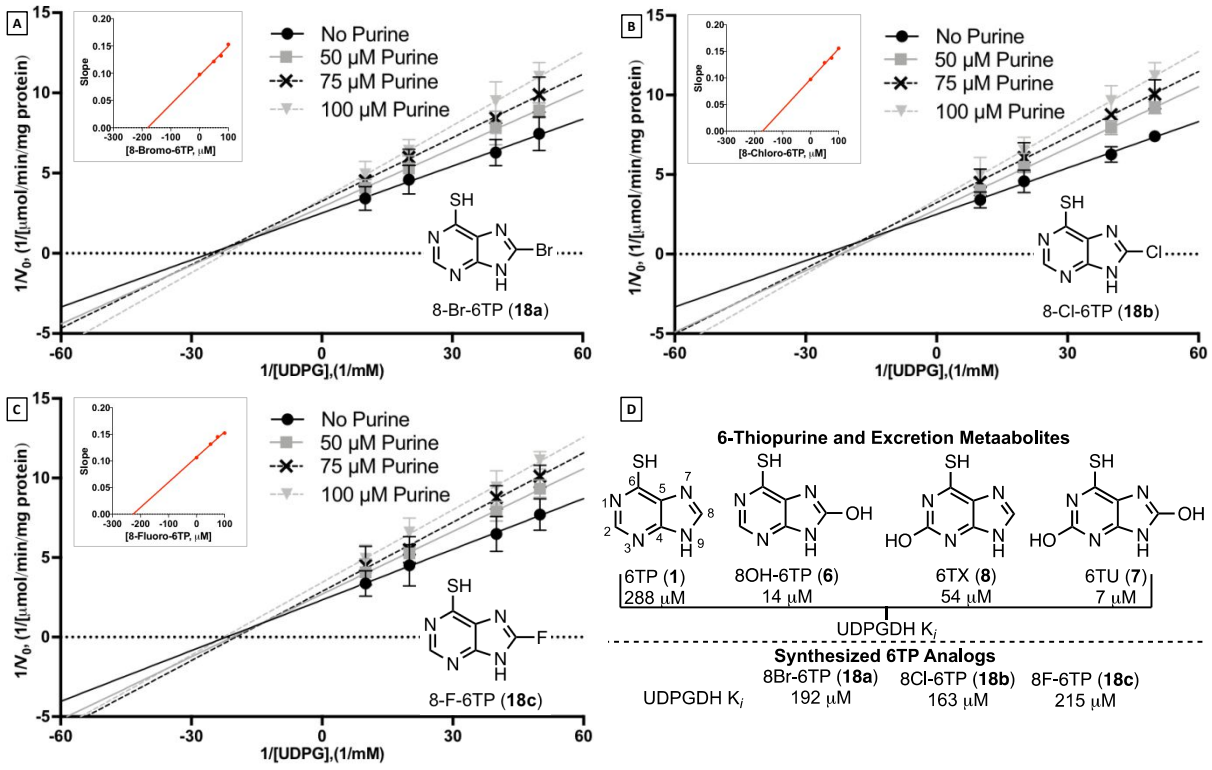

2.3.2 Inhibition Evaluation Towards UGT-1A

While neither 6TP or any of its oxidative metabolites were shown to have inhibition properties toward UGT-1A, the same cannot be assumed for the constructed analogs and, as such, assessment is required. To accomplish this, we employed our previously reported *in vitro* HPLC method for the assessment of UGT-1A inhibition.[31] In this method, the levels of BDG formation is lower than physiological levels given the incubation time (45-minutes). The control showed expected production of BMG exceeding that of BDG. The evaluation of conjugation in the presence of 75 μM 6TP and 75 μM 6TU, independently, showed similar patterns of UCB, BMG, BDG levels with respect to the control group, thus, indicating no inhibition by either purine towards UGT-1A, similar to what was previously reported and observed (Table 3). Similar to the control group and both 6TP and 6TU, each of the analogs were observed to have the same pattern of bilirubin levels. As such, no inhibition towards UGT-1A was observed with any of the 6TP analogs constructed in

this study. Validation of UGT-1A activity was accomplished with the use of regorafenib, previously mentioned as a selective inhibitor of UGT-1A, which showed nearly full inhibition of UGT-1A.

Table 3 Inhibition studies of UGT-1A by 6TP, 6TU, regorafenib, and the three C8-halogenated 6TP analogs. Quantification of unconjugated bilirubin (UCB), monoglucuronide bilirubin (BMG, sum of BMG1 and 2), and diglucuronide bilirubin (BDG) accomplished via the bilirubin standard curve (see supplemental information). Each group is an average of three independent runs with standard error bars shown.

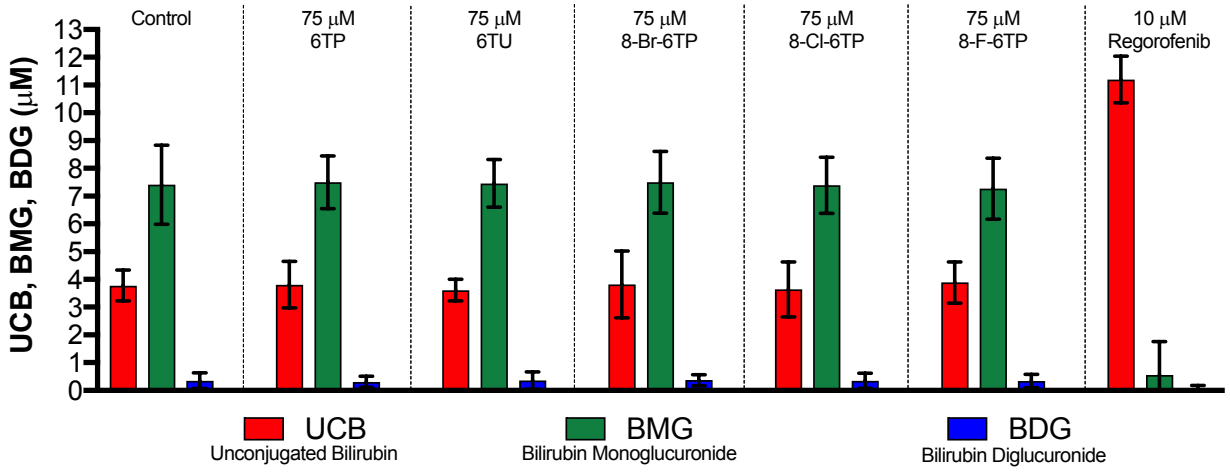

2.3.4 Cytotoxicity Evaluation against REH

While the C8-halogenated analogs were shown to possess weak inhibition towards UDPGDH and no inhibition towards UGT-1A, investigations into the possible retention of cytotoxicity was undertaken. To explore the analogs cytotoxic properties, each analog, 6TP, 6TX, 8-OH-6TP, 6TU, and doxorubicin (control) was evaluated towards the acute lymphocytic leukemia cell line, REH, over a 48-hour period. Cytotoxicity was assessed via cellular viability, Alamar blue quantification, over 48 h and data was analyzed via Prism 7.0 by GraphPad Pro. 6TP was shown to have an IC_{50}

of 2.94 μM (±0.48) and doxorubicin of 0.285 (±0.008) as shown in Table 4. Neither 6TU nor 6TX, both C2 hydroxylated purines, were observed to have cytotoxicity below 10 μM in the REH cancerous cell line. It is thought that the lack of cytotoxicity by these two oxidative metabolites arises from the hydroxyl at the C2 position, thus preventing phosphoribosylation by HGPRT and ultimate formation of dTGTP (**4**). While the C2 position of TIMP does undergo C2 hydroxylation followed by amine installation, these steps are performed upon the nucleotide variant of 6TP and not the free 6TP nitrogenous base form. Furthermore, the affinity of 6TU and 6TX towards UDPGDH could be stronger than that of HGPRT, thus preventing formation of **4**. In comparison, the C8 hydroxyl of 8-OH-6TP was observed to be cytotoxic, possessing an IC_{50} value of 9.91 μM (±2.36). This suggests that substitution about the C8 position is tolerable, and, most importantly, could translate into retention of cytotoxicity. Each of the analogs were shown to possess cytotoxicity, with IC_{50} values of: **18a** (C8 Br) 9.54 μM (±0.97), **18b** (C8 Cl) 3.95 μM (±1.94), and **18c** (C8 F) 4.71 μM (±1.40).

It is assumed that the cytotoxicity of these analogs arise from their incorporation into DNA, in a similar pathway and sequence to that of 6TP, but this has not been proven in this study. Assuming the same mode of action as 6TP, the observed lower potency of the bromine compared to the chlorine and fluorine analogs is thought to arise from its size. The size of bromine upon the C8 position of the purine within the deoxyguanosine mimic could hinder DNA incorporation. Similarly, the increase bulk of the bromine upon the C8 position could prevent enzymatic recognition by the HGPRT, as well as, the other enzymatic steps leading to the formation of **4**. The increased cytotoxicity observed by both the chlorine and fluorine analogs lend further support to the possible role of size in the observed trend of cytotoxicity. However, the greater cytotoxicity exhibited by the chlorine analog versus the fluorine analog contradicts the argument of size as a

function of activity, but could also lead to an electronic argument for activity. Further investigations are required to fully understand the observed trend. Most importantly, through these analogs it was shown that substitution of the C8 position is not only tolerated, but does give access to 6TP analogs that retain cytotoxicity.

Table 4 Evaluation of 6TP, excretion metabolites, and synthesized 8-substituted analogs towards inhibition of UDPGDH and UGT-1A and cytotoxicity towards REH (acute lymphocytic leukemia) cancerous cell lines. All experiments were carried out in triplicate and standard error is reported.

Compound	IC_{50} (μM) REH
6TP	2.94 (±0.48)
6TU	>10
6TX	>10
8-OH-6TP	9.91 (±2.36)
18a (Br)	9.54 (±0.97)
18b (Cl)	3.95 (±1.94)
18c (F)	4.71 (±1.40)
Doxorubicin	0.285 (±0.08)

3. Conclusions

Through this study, further investigations into the mode of toxicity associated with the therapeutic application of 6-thiopurine has been accomplished. It has been found that inhibition of UDPGDH, one of two critical steps in the bilirubin pathway, is highly inhibited by 6TU, the primary excretion metabolite of 6TP. Based upon previous structure-activity relationships of the excretion metabolites of 6TP, it was postulated that substitution about the C8 position could decrease inhibition towards UDPGDH while retaining its cytotoxic character. The synthesis of the C8 substituted bromine, chlorine, and fluorine analogs were successfully accomplished from 6-chloropurine in 32%, 22%, and 16% yields, respectively, all over five synthetic steps. Each of the

analogs were shown to have low inhibition (192, 163, 215 μM, respectively) towards UDPGDH, similar to 6TP (288 μM) and no inhibition towards UGT-1A. The C8-bromo analog had limited cytotoxicity towards the acute lymphocytic leukemia cell line REH, IC_{50} of 9.54 μM, however the chloro- and fluoro-6TP analogs were shown to retain cytotoxicity with IC_{50} values of 3.95 and 4.71 μM, respectively. These results have effectively shown that structural modifications of 6-thiopurine will not only retain cytotoxicity, but also decrease inhibition towards UDPGDH, a critical step found to be responsible for the most predominate toxic side effects of 6TP administration. It is anticipated that with a decrease in toxicity of new 6TP analogs, an increase in dosage can be administered, resulting in further increase of therapeutic properties of 6TP treatment. As such, newly constructed analogs of 6TP will lead to a more potent anti-leukemic drug that can help maintain the quality of life for patients through decreased associated toxicities.

4. Experimental Section

4.1 Chemistry

All reagents were commercially available and used without purification unless otherwise stated. NMR spectra were recorded with a Varian 400 MHz instrument. The chemical shifts are given in parts per million (ppm) relative to residual $CHCl_3$ at δ 7.26 ppm or DMSO δ 2.50 ppm for proton spectra and relative to $CDCl_3$ at δ 77.23 ppm or DMSO δ 39.52 ppm for carbon spectra, unless otherwise noted. Low-resolution mass spectra were obtained using a Waters Xevo-TQD via direct injection; samples were dissolved in methanol, filtered, and the supernatant injected. Flash column chromatography was performed with silica gel grade 60 (230-400 mesh). Dichloromethane (CH_2Cl_2), tetrahydrofuran (THF), toluene (PhMe), *N,N*-dimethylformamide (DMF), and

acetonitrile (CH_3CN) were all degassed with argon and passed through a solvent purification system containing alumina or molecular sieves. All commercially available reagents were used as received. All procedures including anhydrous solvents were performed with rigorously dried glassware under inert atmosphere.

4.1.1. Synthesis of 6-chloro-9-(4-methoxybenzyl)-9*H*-purine (14). To a stirring solution of 6-chloropurine (**13**; 1.5 g, 9.6 mmol, 1.0 eq.) in DMF (30 mL) was added K_2CO_3 (2.7 g, 19.2 mmol, 2.0 eq.) and *para*-methoxybenzyl chloride (1.44 g, 10.6 mmol, 1.1 eq.) and left to stir for 20 h. The reaction was quenched with the addition of water (1 vol. eq.) and the product was extracted with EtOAc (x3). The organic layers were combined, wash with brine, dried over sodium sulfate, and concentrated under reduced pressure. The crude material was purified via flash silica gel chromatography (gradient elution EtOAc:hexane of 1:2 to 9:1) to afford **14** (1.55 g, 58% yield) and **15** (0.9 g, 34% yield). ^{1}H NMR (DMSO, 400 MHz) δ (ppm): 8.81 (s, 1H), 8.78 (s, 1H), 7.33 (d, J = 8.0 Hz, 2H), 6.89 (d, J = 8.1 Hz, 2H), 5.43 (s, 2H), 3.70 (s, 3H). ^{13}C NMR (DMSO, 101 MHz) δ (ppm): 159.8, 152.3, 149.8, 148.0, 145.3, 131.5, 130.1, 128.6, 114.8, 55.8, 47.3. LRMS (ESI): *m/z* calcd for $C_{13}H_{11}ClN_4NaO$: $[M+ Na]^+$ 297.05, found 297.12.

4.1.2. General procedure for the synthesis of 8-substituted 6-chloro-9-(4-methoxybenzyl)-9*H*-purine analogs (16a-c). To a mixture of anhydrous diisopropyl amine (1.3 eq.) in THF (0.3 M) at -78 °C, under an argon atmosphere, was slowly added *n*-BuLi (1.6 M, 1.3 eq.) over 5 min. After 45 min of stirring at -78 °C purine **14** (1 eq.) in THF (0.1 M) was added slowly, followed by 2.5 eq. of a prepared 1 M anhydrous solution of halogenating reagent in THF over 15 min. The mixture was allowed to room temperature slowly, and was then quenched with saturated ammonium chloride, and the product was extracted with CH_2Cl_2 (x3). The organic layers were

combined, dried over sodium sulfate, and concentrated under reduced pressure. Product purification is described below.

4.1.2.1. 8-Bromo-6-chloro-9-(4-methoxybenzyl)-9H-purine (**16a**): The crude material was purified via flash silica gel chromatography (Et_2O:hexane 1:1) to afford **16a** in 75% as a yellowish amorphous solid (mp: 115-117). ^{1}H NMR (DMSO, 400 MHz) δ (ppm): 8.81 (s, 1H), 7.23 (d, J=8.4 Hz, 2H), 6.88 (d, J=8.4 Hz, 2H), 5.41 (s, 2H), 3.70 (s, 3H). ^{13}C NMR (DMSO, 101 MHz) δ (ppm): 159.7, 153.6, 152.7, 148.3, 136.2, 131.8, 129.6, 127.6, 114.9, 55.8, 47.9. LRMS (ESI): *m/z* calcd for $C_{13}H_{10}ClBrN_4NaO^+$: [M+Na^+] 374.96, found 375.08.

4.1.2.2. 6,8-Dichloro-9-(4-methoxybenzyl)-9H-purine (**16b**): The crude material was purified via flash silica gel chromatography (Et_2O:hexane 3:1) to afford **16b** in 70% yield as a white amorphous solid (mp: 111-113 °C). ^{1}H NMR (DMSO, 400 MHz) δ (ppm): 8.84 (s, 1H), 7.26 (d, J = 8.5 Hz, 2H), 6.88 (d, J = 8.5 Hz, 2H), 5.42 (s, 2H), 3.70 (s, 3H). ^{13}C NMR (DMSO, 101 MHz) δ (ppm): 159.5, 152.2, 152.1, 149.6, 147.8, 131.3, 129.9, 128.4, 114.6, 55.6, 47.1. LRMS (ESI): *m/z* calcd for $C_{13}H_{10}Cl_2N_4NaO^+$: [M+Na^+] 331.01, found 331.04.

4.1.2.3. 8-Fluoro-6-chloro-9-(4-methoxybenzyl)-9H-purine (**16c**): The crude material was triturated in diethyl ether and filtered (x2) to afford **16c** in 71% yield as a white apmorphous solid (mp: 110-112). ^{1}H NMR (DMSO, 400 MHz) δ (ppm): 8.99 (s, 1H), 7.23 (d, J = 8.5 Hz, 2H), 6.72 (d, J = 8.5 Hz, 2H), 6.06 (s, 2H), 3.63 (s, 3H). ^{13}C NMR (DMSO, 101 MHz) δ (ppm):159.7, 152.7, 146.5, 139.2 & 136.26 (C8), 131.8, 127.6, 114.9, 105.0, 55.8, 47.9. LRMS (ESI): *m/z* calcd for $C_{13}H_{10}ClFN_4NaO^+$: [M+Na^+] 315.04, found 315.03.

4.1.3. General procedure for thiol installation (17a-c). To a stirring solution of **16** (1 eq.) in MeCN (0.15 M) under an argon atmosphere was added thiourea (2 eq.) and brought to reflux for 2 h. The solvent was removed under reduced pressure to afford the thiourea purine, to which was

added ethanol (1.5 volume equivalents) and refluxed. After 2 h, the reaction mixture was allowed to cool to room temperature, and purification for each compound is described below.

4.1.3.1. 8-Bromo-9-(4-methoxybenzyl)-9H-purine-6-thiol (**17a**): Once at room temperature, the resulting yellow crystals were filtered via vacuum filtration, washed with diethyl ether, and left to dry over night to afford **17a** (181 mg 92% yield) as a white amorphous solid. ^{1}H NMR (DMSO, 400 MHz) δ (ppm): 13.52 (bs, 1H), 8.23 (s, 1H), 7.31 (d, J = 8.4 Hz, 2H), 6.85 (d, J = 8.5 Hz, 2H), 5.26 (s, 2H), 3.70 (s, 3H). ^{13}C NMR (DMSO, 101 MHz) δ (ppm): 169.5, 164.5, 159.4, 147.1, 144.0, 130.1, 128.5, 125.9, 114.5, 55.8, 45.6. LRMS (ESI): *m/z* calcd for $C_{13}H_{11}BrN_4NaOS^+$: [M+ Na^+] 372.97, found 372.95.

4.1.3.2. 8-Chloro-9-(4-methoxybenzyl)-9H-purine-6-thiol (**17b**): Once at room temperature, the resulting yellow crystals were filtered via vacuum filtration, washed with diethyl ether, and left to dry over night to afford **17b** (177 mg 89% yield) as a white amorphous solid. ^{1}H NMR (DMSO, 400 MHz) δ (ppm): 13.51 (s, 1H), 8.23 (s, 1H), 7.31 (d, J = 8.5 Hz, 2H), 6.85 (d, J = 8.5 Hz, 2H), 5.26 (s, 2H), 3.69 (s, 3H). ^{13}C NMR (DMSO, 101 MHz) δ (ppm): 169.3, 164.2, 159.2, 147.0, 143.8, 129.8, 128.3, 125.6, 114.3, 55.5, 45.4. LRMS (ESI): *m/z* calcd for $C_{13}H_{11}ClN_4NaOS^+$: [M+ Na^+] 329.02, found 328.99.

4.1.3.3. 8-Fluoro-9-(4-methoxybenzyl)-9H-purine-6-thiol (**17c**): Once at room temperature, the resulting yellow crystals were filtered via vacuum filtration, washed with methanol, and left to dry over night to afford **17c** (181 mg 92% yield) as a white amorphous solid. ^{1}H NMR (DMSO, 400 MHz) δ (ppm): 13.51 (s, 1H), 8.27 (s, 1H), 7.25 (d, J = 8.4 Hz, 2H), 6.82 (d, J = 8.4 Hz, 2H), 5.26 (s, 2H), 3.61 (s, 3H). ^{13}C NMR (DMSO, 101 MHz) δ (ppm): 176.5, 159.1, 149.9, 145.9, 140.5 & 134.9 (C8), 130.1, 128.9, 114.1, 110.0, 55.4, 47.2. LRMS (ESI): *m/z* calcd for $C_{13}H_{11}FN_4NaOS^+$: [M+ Na^+] 313.05, found 313.05.

4.1.4. General procedure for PMB deprotection. Under the protection of an argon atmosphere, concentrated sulfuric acid (2 eq.) was added drop wise to a stirring solution of **17** (1 eq.) in PhMe (0.085 M) and allowed to stir. After 2.5 h, the reactions were purified via the procedures described below.

4.1.4.1. 8-Bromo-9H-purine-6-thiol **(18a**): The PhMe was decanted off, and the residue was triturated with Et_2O and filtered via vacuum filtration to obtain red/orange crude crystals. The water-soluble impurities were removed by partially dissolving the material in water, gently heating the mixture, and then allowed to cool to room temperature. The resulting yellow crystals that formed were collected by vacuum filtration and washing with Et_2O to obtain **18a** in 81% yield. ^{1}H NMR (DMSO, 400 MHz) δ (ppm): 13.70 (bs, 1H), 8.50 (s, 1H). ^{13}C NMR (DMSO, 101 MHz) δ (ppm): 176.2, 165.0, 148.7, 137.4, 133.1. LRMS (ESI): *m/z* calcd for $C_5H_3BrN_4NaS^+$: $[M+ Na]^+$ 252.92, found 252.92.

4.1.4.2. 8-Chloro-9H-purine-6-thiol **(18b**): The PhMe was decanted off, and the residue was triturated with Et_2O and filtered via vacuum filtration to obtain the crude crystals. The water-soluble impurities were removed by partially dissolving the material in water, gently heating the mixture, and then allowed to cool to room temperature. The resulting white crystals that formed were collected by vacuum filtration and washing with Et_2O to obtain **18b** in 62% yield. ^{1}H NMR (DMSO, 400 MHz) δ (ppm): 13.71 (bs, 1H), 13.51 (bs, 1H), 8.52 (s, 1H). ^{13}C NMR (DMSO, 101 MHz) δ (ppm): 177.5, 165.3, 148.5, 135.1, 131.9. LCMS (ESI): *m/z* calcd for $C_5H_3ClN_4NaS^+$: $[M+ Na]^+$ 208.97, found 208.91.

4.1.4.3. 8-Fluoro-9H-purine-6-thiol **(18c**): The PhMe was decanted off, and the residue was triturated with Et_2O and filtered via vacuum filtration to obtain the crude crystals. The resulting solid was then dissolved in a minimum amount of warm ethanol, followed by a slow addition of

$NaHCO_{3\ (aq)}$ forming a pale-yellow cloudy solution. Dropwise addition of 1 M $HCl_{(aq)}$ to a pH of 2.5 gave a transparent solution that upon cooling to 0 °C afforded yellow/orange crystals, which were filtered and rinsed with cold ethanol (x3) and left to dry to obtain **18c** in 41% yield. ^{1}H NMR ($DMSO_3$, 400 MHz) δ (ppm): 13.68 (bs, 1H), 12.42 (bs, 1H), 8.28 (s, 1H). ^{13}C NMR (DMSO, 101 MHz) δ (ppm): 177.1, 168.9, 159.2, 153.1 & 149.9 (C8), 133.7. LCMS (ESI): *m/z* calcd for $C_5H_3FN_4NaS^+$: $[M+ Na]^+$ 193.00, found 192.97.

4.2. Biological

4.2.1. UDP-Glucose Dehydrogenase Inhibition Assay

Inhibitor Assessment – General Procedure: Spectrometric analysis was performed on a Hewlett-Packard 8452 Diode Array UV/Vis spectrometer equipped with a Lauda Brinkman Ecocline RE 106 E100 circulating water bath. The water bath was maintained at 25 °C and the diode array was set at 340 nm, both were allowed to warm up 10-minutes prior to analysis. To a 1 mL cuvette, 300 mL of 0.5 M Gly-Gly (0.15 M final concentration), nanopure water, varying NAD^+ and UDPG concentration in varying inhibitor concentrations were added and placed in the diode array for a 2 min thermal equilibration. Once 1.5 minutes elapsed, the instrument was zeroed to obtain an initial rate change in absorbance versus time. The reaction was initiated by addition of 20 μL of the UDPGDH solution. Thorough mixing by inversion of the cuvette was performed as quickly as possible and then placed in the holder for analysis. The reaction was monitored from 20 to 120 seconds after enzyme addition, and the slope was calculated from 20 to 40 seconds using the diode array software.

4.2.1.1 Inhibitor Assessment – Saturating NAD^+ varying UDPG concentration: For each analysis, the cuvette was prepared in the same fashion as outlined above. The final concentration

of the components of the mixture were 150 mM Gly-Gly, 0.1 unit/mL UDPGDH, 3 mM NAD^+ and varied concentrations of 0.1, 0.05, 0.025 and 0.02 mM of UDPG, obtained from stock solution addition. Nanopure water was used as a variable component to ensure that a final volume of 1 mL was obtained. Inhibitor analysis of the four purines was performed at two concentrations: 50 and 100 μM for 6TP, 20 and 50 μM for 6TX and 8OH-6TP, and 5 and 10 μM for 6TU, obtained from their corresponding stock solutions. Each assessment was performed in triplicate. The average of the three were plotted and the slopes were used to determined inhibition values.

4.2.2. UDP-glucuronosyltransferase activity assay

4.2.2.1. Quantification of Bilirubin, and Mono/Di-glucuronide Levels: Bilirubin was quantified directly from the generated standard curve (see Supplementary Information). A total of ten peaks for the glucuronide species, including their isomers were detected in the incubation samples. Peak assignment and identification of UCB, BMG1, BMG2, BDG and their isomers were based on their lipophilicity and polarity, as well as the elution pattern, chromatographic peak position and relative retention time from previous reports.[21-23, 42] The calibration curves for bilirubin were used to determine the concentration of the mono- and di-glucuronide species employing the gradient HPLC bilirubin method described above. Quantification of UDPGA levels was determined through the use of the constructed standard curve within the isocratic HPLC method developed for UDGPA.

Bilirubin Glucuronide Formation: Bilirubin glucuronidation was performed at 37 °C in a shaking water bath. All steps taken were performed in the lowest light conditions possible; the glucuronide formed was found to be unstable to ambient lighting. The following was added to an Eppendorf tube to achieve the final concentrations indicated, final volume 200 μL: potassium phosphate buffer (50 mM, pH 7.4), bilirubin (10 μM), $MgCl_2•6H_2O$ (0.88 mM), rat liver

microsomes (RLM, 100 μg of protein/mL), alamethicin (22 μg/mL), and allowed to pre-incubated for 2 min. Addition of UDPGA (3.5 mM), referred to as the zero-time point, initiated the reaction. The mixture was allowed to shake at 37 °C for each of the time course experiments. To each reaction 600 μL of ice-cold methanol containing 200 mM ascorbic acid was added to terminate the enzymatic reaction, vortexed for 2 min, and then centrifuged at 12,000 rpm for 10 min. The supernatant was then analyzed by the developed gradient HPLC protocol for separation and quantification of UCB, BMG1, BMG2, and BDGs.

Validation of Bilirubin Glucuronide Formation: Quantification of UCB, BMG1&2 and BDGs were performed post the quenching of UGT1A1, which was performed by immersing the Eppendorf tube with the reaction mixture in a cold-water bath for two min. No ascorbic acid was used, as the residual material would quench the glucuronidase enzyme to be added. To this sample 0.1 mg/mL glucuronidase enzyme was added, inverted (x3), and then analyzed by the HPLC protocol developed to quantify the levels of bilirubin and BMG1&2 and BDGs for formation confirmation.

4.2.2.2. Inhibitor Assessment of Bilirubin Glucuronide Formation: Employing the same protocol delineated above for the formation of the bilirubin glucuronide species, inhibitor assessment was performed. To the Eppendorf tube, the purine (50 and 75 μM final concentrations) was added alongside a control (no purine added) and allowed to pre-incubate for 2 min. Addition of UDPGA initiated the reaction for each of the time course experiments. The gradient HPLC method was employed for the 45-min time course experiments for the quantification of the glucuronide species.

4.2.3. IC_{50} Value Determination in REH using Alamar Blue Quantification

The acute lymphocytic leukemia cell line REH was grown in media supplemented with fetal bovine serum (FBS) and antibiotics (100 μg/mL penicillin and 100 U/mL streptomycin). Cells were incubated at 37 °C in a 5% CO_2, 95% humidity atmosphere. Cellular viability was determined by quantification via Alamar blue.

General Procedure: Compounds were solubilized in DMSO (10 μM stock solutions) and added to a 96-well plate over a range of concentrations (31.6 nM to 200 μM) with media, and 40 μL was added to the 384-well plate in triplicate for each concentration of compound. Cells were then added to the plate (2,000 cells/well) in 10 μL of media. After 69 h of continuous exposure, 5 μL of Alamar Blue was added to each well, and the cells were allowed to incubate for an additional 3 h. The plates were then read for fluorescence intensity with an excitation of 560 nm and emission of 590 nm on a BioTek Synergy H1 plate reader. Doxorubin and etoposide were both used as positive death controls, and wells with no compounds added as negative death controls. IC_{50} values were determined from three or more independent experiments using GraphPad Prism 7.0. (LaJolla, CA, USA)

4.2.4 Investigations into UDPGDH Inhibition by 6TP and 6TU in Hepatocytes

A male Sprague-Dawley rat was housed in an animal care room, kept at 25 °C with a 12 h light/dark cycle, and had free access to food and water. The rat was anesthetized by IP injection of ketamine/xylazine mixture (ketamine 100 mg/kg and xylazine at 15 mg/kg). Rat hepatocytes were isolated through the procedure outlined by Ogimura[43] and Ito.[44] Through the portal vein and inferior vena cava was inserted an IV cannula. The liver was washed with a perfusion solution (Ca^{2+} free, EDTA-containing perfusion buffer) for 10 min, followed by a perfusion with a collagenase containing buffer. Hepatocytes were isolated, filtered through a sterile nylon mesh, and purified via a Percoll solution, and washed with WME media (comprised of 10% FBS, 5%

penicillin and streptomycin, and 22 μg/mL alamethicin). Hepatocyte viability was assessed by Trypan blue exclusion, and cells with viabilities of >90% were used for the study. Cells were seeded onto a collagen-coated tissue culture plate, density of 500,000 cells/well, in 1 mL of WME media in a 12-well plate and incubated at 37 °C in a 5% CO_2, 95% humidity atmosphere. Following the procedure established by Ito,[44] cell media was exchanged and the hepatocytes were left to grow for 5 days.

Assessment: Hepatocytes were transferred to a 24-well plate (20,000 cells/well) in 500 of HWE media and allowed to adhere for 24 h. The media was removed and replaced with 1 mL of a buffer solution comprised of: HWE, bilirubin (10 μM), $MgCl_2$•$6H_2O$ (0.88 mM), alamethicin (22 μg/mL), and 15 μM UDPG and left to incubate. To this buffered solution was added the purines of interest, as well 15 μM UDPGA and 10 μM of regorafenib. The addition of the buffered solution was considered the 0-min time point. After 24 h, the liquid mixture was transferred to labelled Eppendorf tubes and 2 mL of trypsin was added to well and left to incubate for 20 min at which 4 mL of WME media was added. The 6 mL of the cell mixture was then centrifuged (10,000 g, 2 min), the supernatant removed, washed three times with PBS buffer via gentle resuspension and centrifugation. The pellet was treated with 0.7 mL of a lysis solution (ETA, SDS, Tris HCl at pH 8.00) and 600 μL of ice-cold methanol containing 200 mM ascorbic acid was added to terminate the enzymatic reaction, vortexed for 2 min, centrifuge at 20,0000 x g for 15 min (pellet large cellular debris), the supernatant was added to the original liquid and assessed for UCB, BMG, and BDG levels via the HPLC previously described.

Ethics statement

All animal experiments were conducted under the supervision of Kansas State University Institutional Animal Care and Use Committee (IACUC) and were conducted according to approved protocols in accordance with all applicable federal, state, local and institutional laws or guidelines governing animal research.

Conflicts of interest

The authors declare no conflict of interest.

Acknowledgements

This work could not have been undertaken without the gracious financial support from the Johnson Cancer Research Center of Kansas State University and Startup Capital from Kansas State University. Funding for this research was provided by the NSF REU program under grant number *CHE-1460898*. A.X.T.H. was supported by the NSF-REU program.

References

1. G. H. Hitchings and G. B. Elion, *Pharmacological Reviews*, 1963, **15**, 365-405.
2. J. M. Torpy, C. Lynm and R. M. Glass, *JAMA*, 2009, **301**, 452-452.
3. T. Moriyama, R. Nishii, T.-N. Lin, K. Kihira, H. Toyoda, N. Jacob, M. Kato, K. Koh, H. Inaba and A. Manabe, *Pharmacogenetics and genomics*, 2017, **27**, 236-239.
4. O. Eden, *Journal of clinical pathology*, 2000, **53**, 55-59.
5. C. Vendrik, J. Bergers, W. De Jong and P. Steerenberg, *Cancer chemotherapy and pharmacology*, 1992, **29**, 413-429.
6. C. Cuffari, E. Seidman, S. Latour and Y. Theoret, *Can. J. Physiol. Pharmacol.*, 1996, **74**, 580-585.
7. D. S. Rampton, *BMJ: British Medical Journal*, 1999, **319**, 1480.
8. M. L. Seinen, D. P. van Asseldonk, N. K. de Boer, N. Losekoot, K. Smid, C. J. Mulder, G. Bouma, G. J. Peters and A. A. van Bodegraven, *Optimalisation of conventional therapies in inflammatory bowel disease*, 2016, **7**, 812-819.
9. X. Roblin, L. P. Biroulet, J. M. Phelip, S. Nancey and B. Flourie, *The American journal of gastroenterology*, 2008, **103**, 3115.

10. R. B. Gearry and M. L. Barclay, *Journal of gastroenterology and hepatology*, 2005, **20**, 1149-1157.
11. J. A. Nelson, J. W. Carpenter, L. M. Rose and D. J. Adamson, *Cancer Research*, 1975, **35**, 2872-2878.
12. S. Haglund, J. Taipalensuu, C. Peterson and S. Almer, *British Journal of Clinical Pharmacology*, 2008, **65**, 69-77.
13. K. Rowland, L. Lennard and J. S. Lilleyman, *Xenobiotica*, 1999, **29**, 615-628.
14. D. M. Tidd and A. R. P. Paterson, *Cancer Research*, 1974, **34**, 738-746.
15. P. Karran and N. Attard, *Nat Rev Cancer*, 2008, **8**, 24-36.
16. P. Karran, *British Medical Bulletin*, 2006, **79-80**, 153-170.
17. L. Chouchana, A. A. Fernández-Ramos, F. Dumont, C. Marchetti, I. Ceballos-Picot, P. Beaune, D. Gurwitz and M.-A. Loriot, *Genome Medicine*, 2015, **7**, 37.
18. T. Dervieux, J. G. Blanco, E. Y. Krynetski, E. F. Vanin, M. F. Roussel and M. V. Relling, *Cancer Research*, 2001, **61**, 5810-5816.
19. T. Dervieux, T. L. Brenner, Y. Y. Hon, Y. Zhou, M. L. Hancock, J. T. Sandlund, G. K. Rivera, R. C. Ribeiro, J. M. Boyett, C.-H. Pui, M. V. Relling and W. E. Evans, *Blood*, 2002, **100**, 1240-1247.
20. J. M. Carethers, M. T. Hawn, D. P. Chauhan, M. C. Luce, G. Marra, M. Koi and C. R. Boland, *Journal of Clinical Investigation*, 1996, **98**, 199-206.
21. G. Ma, J. Lin, W. Cai, B. Tan, X. Xiang, Y. Zhang and P. Zhang, *J. Pharm. Biomed. Anal.*, 2014, **92**, 149-159.
22. D. Zhang, T. J. Chando, D. W. Everett, C. J. Patten, S. S. Dehal and W. G. Humphreys, *Drug Metabolism and Disposition*, 2005, **33**, 1729-1739.
23. J. Zhou, T. S. Tracy and R. P. Remmel, *Drug Metabolism and Disposition*, 2011, **39**, 322-329.
24. R. Troxler and S. Brown, in *Bilirubin*, CRC Press, 2018, pp. 1-38.
25. L. Weaver, A.-R. A. Hamoud, D. E. Stec and T. D. Hinds, *American Journal of Physiology-Gastrointestinal and Liver Physiology*, 2018.
26. B. H. Billing, in *Bilirubin*, CRC Press, 2018, pp. 85-102.
27. M. Vögelin, L. Biedermann, P. Frei, S. R. Vavricka, S. Scharl, J. Zeitz, M. C. Sulz, M. Fried, G. Rogler and M. Scharl, *PLoS ONE*, 2016, **11**, e0155218.
28. E. A. Hullah, P. A. Blaker, A. M. Marinaki, M. P. Escudier and J. D. Sanderson, *Journal of Oral Pathology & Medicine*, 2015, **44**, 761-768.
29. P. P. Siva, K. M. Murali, A. Deepak, S. Murali, S. Michael and M. Sandhya, *Drug Metabolism Letters*, 2016, **10**, 264-269.
30. N. R. Beattie, N. D. Keul, A. M. Sidlo and Z. A. Wood, *Biochemistry*, 2017, **56**, 202-211.
31. C. J. Weeramange, C. M. Binns, C. Chen and R. J. Rafferty, *J. Pharm. Biomed. Anal.*, 2018, **151**, 106-115.
32. G. B. Elion, E. Burgi and G. H. Hitchings, *JACS*, 1952, **74**, 411-414.
33. R. Sariri and G. Khalili, *Russ. J. Org. Chem.*, 2002, **38**, 1053-1055.
34. Z. Luo, Z. Jiang, W. Jiang and D. Lin, *The Journal of Organic Chemistry*, 2018, **83**, 3710-3718.
35. M. Brændvang and L.-L. Gundersen, *Biorg. Med. Chem.*, 2007, **15**, 7144-7165.
36. L.-L. Gundersen, J. Nissen-Meyer and B. Spilsberg, *J. Med. Chem.*, 2002, **45**, 1383-1386.
37. S. H. Jung, G.-S. Hwang, S. I. Lee and D. H. Ryu, *The Journal of organic chemistry*, 2012, **77**, 2513-2518.

38. J. Bergman and L. Venemalm, *The Journal of Organic Chemistry*, 1992, **57**, 2495-2497.
39. A. K. Ghosh, P. Lagisetty and B. Zajc, *The Journal of Organic Chemistry*, 2007, **72**, 8222-8226.
40. S. Prekupec, D. Svedružić, T. Gazivoda, D. Mrvoš-Sermek, A. Nagl, M. Grdiša, K. Pavelić, J. Balzarini, E. De Clercq, G. Folkers, L. Scapozza, M. Mintas and S. Raić-Malić, *J. Med. Chem.*, 2003, **46**, 5763-5772.
41. S. Ciro, C. Rubio, K. Estieu-Gionnet, L. Latxague, G. Déléris, R. Bareille, J. Amédée and C. Baquey, *ChemBioChem*, 2002, **3**, 341-347.
42. M. G. Bartlett and G. R. Gourley, *Seminars in Perinatology*, 2011, **35**, 127-133.
43. E. Ogimura, S. Sekine and T. Horie, *Biochem. Biophys. Res. Commun.*, 2011, **416**, 313-317.
44. C. Liu, S. Sekine and K. Ito, *Toxicol. Appl. Pharmacol.*, 2016, **302**, 23-30.

Investigations into the mode of toxicity of 6-thiopurine has led to the construction of three new analogs that retain efficacy with decreased toxicity.